PNAS
www.pnas.org

Supplementary Information for

Nanobody-based CAR T cells that target the tumor microenvironment inhibit the growth of solid tumors in immunocompetent mice

Yushu Joy Xie[a,b], Michael Dougan[c], Noor Jailkhani[d], Jessica Ingram[e,h], Tao Fang[a], Laura Kummer[a], Noor Momin[b,d], Novalia Pishesha[a,b], Steffen Rickelt[d], Richard O. Hynes[d,f,g], Hidde Ploegh[a,1]

[a]Program in Cellular and Molecular Medicine, Boston Children's Hospital, Boston, MA, USA 02115
[b]Department of Biological Engineering, Massachusetts Institute of Technology, Cambridge, MA, USA 02138
[c]Division of Gastroenterology, Massachusetts General Hospital, Boston, MA, USA 02114
[d]Koch Institute for Integrative Cancer Research, Massachusetts Institute of Technology, Cambridge, MA, USA 02138
[e]Department of Cancer Immunology and Virology, Dana-Farber Cancer Institute, Boston, MA, USA 02215
[f]Department of Biology, Massachusetts Institute of Technology, Cambridge, MA, USA 02138
[g]Howard Hughes Medical Institute, Chevy Chase, MD, United States
[h]Deceased

[1]To whom correspondence should be addressed:

Email: Hidde.Ploegh@childrens.harvard.edu

This PDF file includes:

Supplementary Materials and Methods
Figs. S1 to S8
References for SI reference citations

www.pnas.org/cgi/doi/10.1073/pnas.1817147116

Supplementary Information Text

Supplementary Materials and Methods

VHH-CAR retroviral design and construction

The CAR T cells were composed of a fluorescent protein tracer linked to a P2A sequence for following transduction. This was followed by a CD8 signal sequence and the VHH domain linked to a CD8 hinge and transmembrane domain. These were connected to a CD28 costimulatory signal and a CD3z activation signal. The CAR constructs are contained in a murine stem cell virus based vector, the XZ vector, which was a gift from the Lodish lab. To generate virus, HEK 293T cells are transfected using Fugene 6 (Promega) with the XZ CAR vector and a pCL-Eco packaging vector. Cloning was carried out in DH5a *E. coli* cells.

T cell isolation and CAR transduction and generation

To generate CAR T cells, CD4 and CD8 T cells were first isolated from mouse splenocytes using a magnetic bead based negative selection (Thermo Fisher Dynabeads Untouched Mouse T cell kit). T cells were activated with anti-mouse CD3 and CD28 overnight in complete RPMI (RPMI supplemented with 10% heat-inactivated fetal bovine serum (IFS), non-essential amino acids, 1mmol/L sodium pyruvate, 2mmol/L L-glutamine, 100 U/ml Penicillin/streptomycin, and 50 umol/L 2-mercaptoethanol) and IL2 (recombinantly, house-made) media and then transduced using the retrovirus generated with the XZ vector mixed with polybrene. T cells were spin-fected twice at 2000g with the virus and polybrene mixture. After two spin-fections, cells were expanded for two days and subsequently used for *in vitro* and *in vivo* assays.

Characterization of VHH surface display and binding

Proper surface display of the CARs on T cells was characterized using a flow cytometry based assay. For the GFP-binding Enh CAR, cells were incubated with GFP to measure binding to successfully transduced cells. For the PD-L1 binding A12 CAR, cells were incubated with recombinant PD-L1 fused to an Fc domain. Binding of PD-L1 was then probed with a fluorescently labelled anti-mouse IgG, a gift from the S. Almo lab. For the EIIIB binding B2 CAR, transduced cells were incubated with recombinant EIIIB protein fused to a GST domain (gift from the Hynes lab). Cells were then probed for EIIIB binding by incubation with rabbit anti-GST and fluorescently labelled anti-Rabbit Ig (Southern Biotech).

In vitro cytotoxicity and activation assays

Cytotoxicity of CAR T cells was shown using various co-culture assays. For Enh CAR activity, plates were coated with GFP overnight and then CAR T cells were cultured on these plates for 48 hours. Supernatants were collected and used for IL2 and IFN□ ELISA measurements (BD Biosciences). The cytotoxicity of the PD-L1 targeted CAR T cells was shown by co-culture with B16 melanoma cells, which express PD-L1 naturally. B16 cells were plated in complete RPMI (Corning) and recombinant murine Il2, and A12 CAR T cells were added to the B16 cells for a 48 hour incubation. T cells were then washed out of the plate using PBS, and the number of remaining viable B16 cells were measured using a Cell Titer Glo assay (Promega). Supernatants of each co-culture were collected to be used of IFN□ ELISA measurements (BD biosciences).

Tumor cell lines

B16F10 cells obtained from the ATCC were used in the animal tumor models and *in vitro* studies.

Cells were maintained in complete RPMI, RPMI 1640 supplemented with 10% heat-inactivated fetal bovine serum (IFS), non-essential amino acids, 1mmol/L sodium pyruvate, 2mmol/L L-glutamine, 100 U/ml Penicillin/streptomycin, and 50 umol/L 2-mercaptoethanol. MC38 was obtained from Kerafast and cells were maintained in Dulbecco's medium supplemented with 10% heat-inactivated fetal bovine serum (IFS), non-essential amino acids, 1mmol/L sodium pyruvate, and 100 U/ml Penicillin/streptomycin. C3.43 cells were a gift from the W. Martin Kast lab, University of Southern California. The C3.43 cell line was maintained in Iscove's modified Dulbecco's medium (IMDM) supplemented with 10% IFS, 100 U/ml penicillin/streptomycin, and 50 umol/L 2-mercaptoethanol.

B16 melanoma model for *in vivo* persistence and proliferation

RAG-/- mice (Jackson laboratory) were inoculated with $5*10^5$ B16 cells subcutaneously in the left flank. After two days, mice were injected with $3.5*10^6$ CAR positive T cells from a 40-50% transduced population. Two weeks after tumor inoculation, spleen, lymph nodes and tumors were collected and stained for CD45, CD3, CD4, CD8, CD11b, and CD11c using antibodies purchased from BioLegend.

Tumor models model for efficacy

To test the efficacy of the PD-L1 targeted CAR T cells, PD-L1 deficient mice were inoculated with either $5*10^5$ cells of B16 wild-type cells or B16 melanoma overexpressing PD-L1 under a CMV promoter. Two days after, mice were treated with A12 CAR T cells or non-specific CAR T cells. A total of three CAR T cell injections was given in combination with a twice weekly i.p. injection of the anti-TRP1 antibody TA99, a gift from the D. Wittrup lab. Tumor measurements were taken by caliper every 1-2 days. Animals were sacrificed following CAC protocols. For the MC38 model, $1*10^5$ cells were inoculated into PD-L1-deficient mice, and 5 days after, mice were treated with either A12 CAR or non-specific CAR T cells. A total of three CAR T cell injections was given, once a week, and tumor measurements were taken by caliper every 1-2 days. To test the efficacy of the EIIIB targeted CAR T cells, $1*10^5$ B16 cells were inoculated into wild-type mice. Four days after, mice were treated with either the B2 CAR T cells, non-specific CAR T cells, or left untreated. In the combination treatments with TA99, the mice were treated with the anti-TRP1 antibody twice weekly. Mice from each treatment group were co-housed to minimize variability due to external factors.

Tumor Immunohistochemistry

C57BL/6 mice were inoculated with B16F10 tumors and left untreated or treated with B2 CAR T cells as described above. Tumors were excised on day 16, formaldehyde-fixed and paraffin-embedded according to standard procedures. Sections were prepared with a Leica RM2255 rotary microtome. Heat-induced epitope-retrieval and immunostaining was performed as recently described in detail (1). Primary antibodies used were: NJB2 (2), CD3 (Abcam), CD4 (Thermo Fisher Scientific), CD8a (Thermo Fisher Scientific), CD31 (Abcam). Both control (no primary antibody) mice and NJB2-stained samples were probed with streptavidin horseradish-peroxidase conjugates (BD Biosciences) as secondary reagent, for all other antibodies the secondary ImmPRESS polymer detection systems was used. Vulcan Fast Red Chromogen Kit 2 (red) and DAB Quanto System (brown) were used as substrates, followed by hematoxylin nuclear counterstain according to the supplier's recommendations. For hematoxylin and eosin (H&E) staining, the Thermo Scientific Shandon Varistain Gemini ES Automated Slide Stainer was used. Image documentation was performed using the Leica Aperio AT2 slide scanner system.

Statistical analysis
All statistical analyses were performed using GraphPad Prism. Survival curves were analyzed using the log rank (Mantel Cox) test. Flow cytometry data were analyzed using two-tailed, unpaired Student t tests, with multiple comparison corrections. Statistical significance was determined using the methods described in results/figure legends considering the Bonferroni correction for comparison between multiple groups.

Analysis of A12 CAR T cells effect in WT mice
A complication that at least for now limits the applicability of anti PD-L1 CAR T cells is their ability to not only target PD-L1 positive tumors, but also the host's own T cells and other cell types that express PD-L1. We discovered that brown adipose tissue is a main site of PD-L1 expression, as detected by PD-L1-specific VHHs used for positron emission tomography. Our results clearly demonstrate the ability of CAR T cells to attack the highly aggressive B16 melanoma, which overexpresses PD-L1. To determine the effect of introducing A12 CAR T cells into WT mice, we generated A12 CAR T cells in the PD-L1-/- background and injected either $18*10^6$, $9*10^6$ or $4.5*10^6$ cells into wildtype and PD-L1-/- mice. One day after injection, mice were sacrificed and lymph nodes, spleens, and brown fat were isolated. Brown fat was digested with collagenase, to form a single cell suspension. Cells from the three organs were stained for CD45, CD3, CD4, CD8, CD11b, CD11c, and PD-L1 using antibodies purchased from BioLegend. Flow cytometry was done on a FACs Fortessa (BD), and analyzed with FlowJo software.

Generation of PD-L1 overexpressing cell lines
B16F10 melanoma cells overexpressing PD-L1 were generated by transiently transfecting B16 melanoma cells with a vector expressing murine cDNA under a CMV promoter. Successfully transfected cells were selected for using hygromycin. PD-L1hi B16 melanoma cells were cultured in complete RPMI and kept under constant selection using hygromycin. Transfected cells showed roughly a two-log-fold increase in PD-L1 compared to WT B16. When cells were cultured for two weeks without the hygromycin selection, PD-L1 expression levels started to approach wildtype levels. Cells were stained using sortagged Alexa-647-conjugated B3, a VHH that binds to the same PD-L1 epitope as A12 (3).

Expansion of A12 and B2 CAR T cells in RAGKO mice
To verify that A12 and B2 CAR T cells can indeed expand, RAG-/- mice were inoculated with B16 tumors and a single injection of either the A12 [$4*10^6$], B2 [$4*10^6$] or 1B7 [$4*10^6$] CAR T cells were introduced. Mice were sacrificed when the tumor area reached $125mm^2$, and the spleen, draining lymph node, and tumors were removed for flow cytometry analysis. Cells were stained for stained for CD45, CD3, CD8, CD4, CD11b and CD11c using antibodies purchased from BioLegend. CAR T cells were tracked by the presence of either GFP or mCherry. All samples were collected on a FACs Fortessa (BD), and analysis was done using FlowJo.

Analysis of anti-VHH immunogenicity of CAR T cells
To determine the extent of anti-VHH immunogenicity developed by three injections of CAR T cells, serum was collected from each treated mouse at the time of sacrifice. Anti-VHH IgG levels were determined by using binding assays, where plates were coated overnight with 1ug/ml of A12 or B2 VHH and then blocked for two hours. Serum from each mouse was added to each well at a 1:100 dilution and the presence of anti-VHH IgGs was detected using an anti-mouse-HRP conjugate (BD Biosciences). To determine the immunogenicity of CAR treatment, the CAR serum

was compared to two different positive, anti-VHH serums controls - one that was actively immunized against A12 using Freund's Complete Adjuvant and another that had been daily injected with 150ug of soluble VHH for multiple weeks. Both the A12 and B2 CAR T cells appear to have low immunogenicity and the level of immunogenicity does not correlate to survival length, suggesting that immunogenicity against VHHs used in the CAR T cells does not have a large impact on survival.

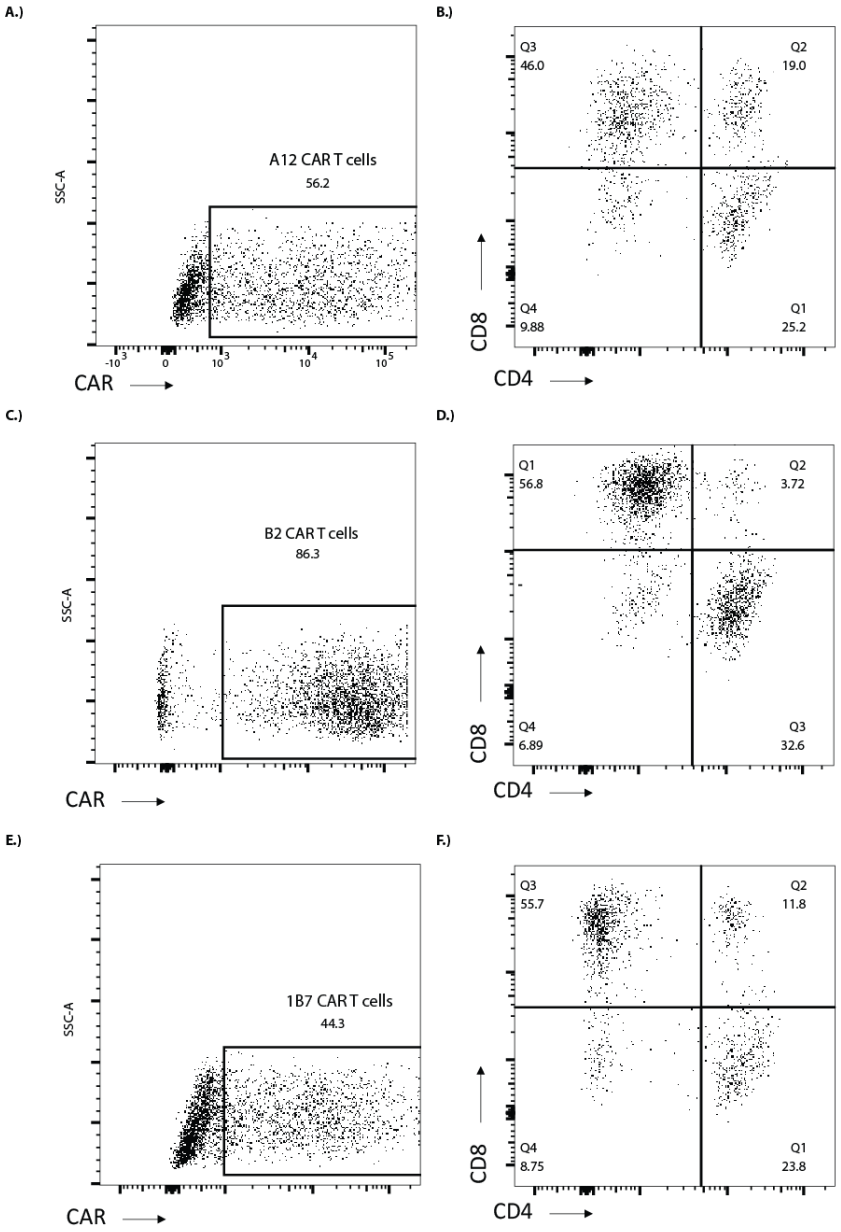

Fig. S1. Primary T cells are effectively transduced with retrovirus encoding VHH-based CAR T cells. (A) The A12 CAR is typically transduced into T cells at around 50% efficiency. After 5 days in culture, the CD8 to CD4 ratio was around 2:1. **(B)** The B2 CAR T cells were transduced at around 85% efficiency as tracked by mCherry expression. The CD8:CD4 ratio was roughly 2:1, similarly to the A12 CAR T cells. **(C)** The 1B7, nonspecifically-targeted CAR T cell, is typically

transduced at around 45% efficiency. Similar to the A12 and B2 CARs, the CD8 T cells expanded preferably under the culture conditions, resulting in a 2:1 CD8:CD4 ratio at the time of injection.

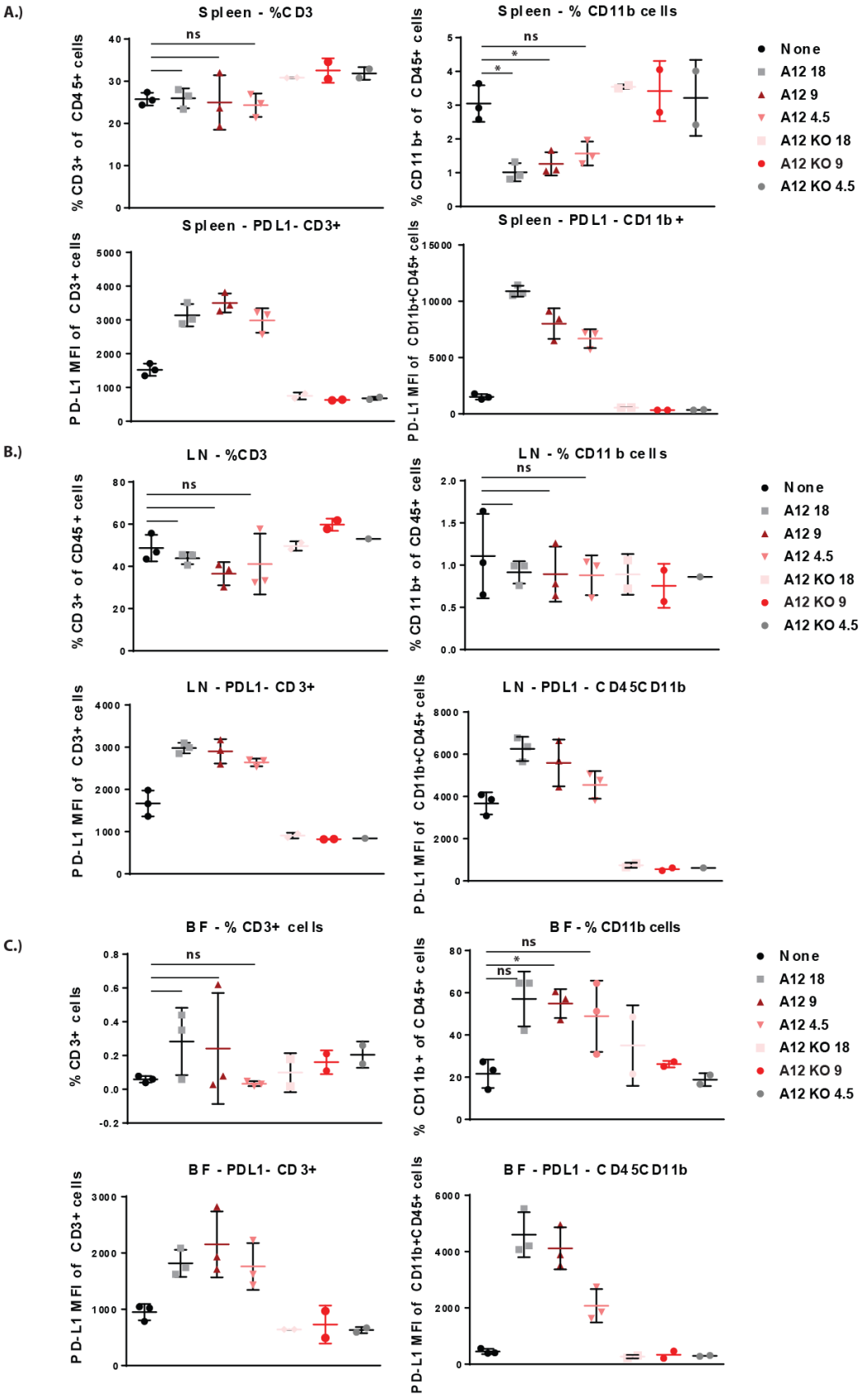
A.)
Spleen - %CD3
% CD3+ of CD45+ cells
ns
Spleen - % CD11b cells
% CD11b+ of CD45+ cells
ns
*
*
Spleen - PDL1- CD3+
PD-L1 MFI of CD3+ cells
Spleen - PDL1 - CD11b+
PD-L1 MFI of CD11b+CD45+ cells
None
A12 18
A12 9
A12 4.5
A12 KO 18
A12 KO 9
A12 KO 4.5
B.)
LN - %CD3
% CD3+ of CD45+ cells
ns
LN - % CD11b cells
% CD11b+ of CD45+ cells
ns
LN - PDL1- CD3+
PD-L1 MFI of CD3+ cells
LN - PDL1 - CD45CD11b
PD-L1 MFI of CD11b+CD45+ cells
None
A12 18
A12 9
A12 4.5
A12 KO 18
A12 KO 9
A12 KO 4.5
C.)
BF - % CD3+ cells
% CD3+ cells
ns
BF - % CD11b cells
% CD11b+ of CD45+ cells
ns
*
ns
BF - PDL1- CD3+
PD-L1 MFI of CD3+ cells
BF - PDL1 - CD45CD11b
PD-L1 MFI of CD11b+CD45+ cells
None
A12 18
A12 9
A12 4.5
A12 KO 18
A12 KO 9
A12 KO 4.5

Fig. S2. Immune population changes due to A12 CAR T cell treatment in wildtype mice. To address the impact of anti-PD-L1 CAR T cells on normal cells and tissues such as lymphocytes and brown adipose tissue, we raised anti-PD-L1 CAR T cells in a PD-L1-/- background and transferred graded numbers of cells [$18*10^6$, $9*10^6$, or $4.5*10^6$] into either WT or PD-L1-/- mice. We tracked the persistence of the transferred cells and recorded the cellular composition of secondary lymphoid organs and brown adipose tissue. We find that CD11b+CD45+ cells appear to be the most effected by anti-PD-L1 CAR T cells, possibly due the higher levels of PD-L1 expression compared to other CD45+ cells, such as CD3+ T cells. **(A)** In the spleen, we see a decrease in CD11b+ cells with increased amounts of A12 CAR T cells injected. We do not see significant changes in the CD3+ population, possibly due to the lower levels of PD-L1 expression. **(B)** In the lymph node, we do not see significant changes in either CD11b or CD3 populations. **(C)** In the brown fat, we see a slight, but not significant, increase in both CD3 and CD11b cells at higher levels of CAR introduction. The CD3 population is expected to increase because brown fat is PD-L1 positive, and we expect infiltration of our CAR T cells. However, the CD11b population in brown fat also increases despite being PD-L1 positive, potentially indicating the tissue becomes inflammatory with an influx of T cells, leading to CD11b cell recruitment. Overall, it appears that the level of PD-L1 expression is correlated to depletion by our A12 CAR T cells.

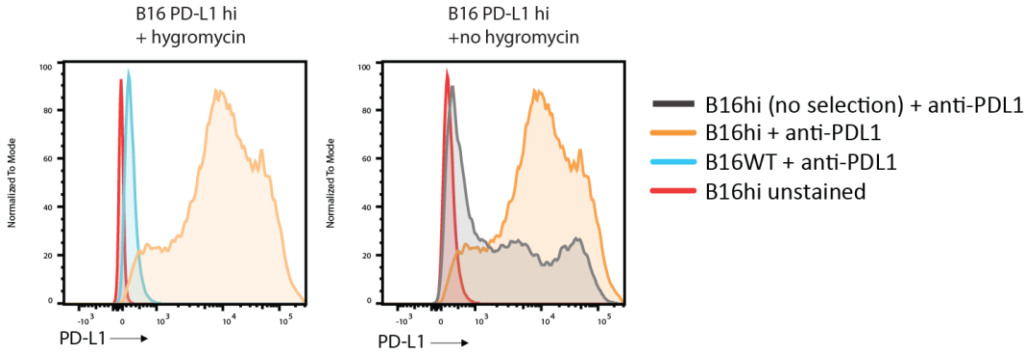

Fig. S3. B16 cells are transfected to overexpress PD-L1. (A) B16 cells are transiently transfected to overexpress PD-L1 under a CMV promoter. Cells are kept under hygromycin selection, and were stained with a PD-L1 targeted VHH labeled with Alexa-647. Transfected cells show around a 2-log-fold increase in PD-L1 expression over B16 wildtype cells. **(B)** PD-L1-overexpressing B16 cells were cultured without hygromycin selection for two weeks and stained for PD-L1 expression. Around 50 percent of cells express 1-2 log-fold higher levels of PD-L1 compared to wildtype cells. We do see loss of PD-L1 expression over time, without selection, and this is reflected in *in vivo* experiments.

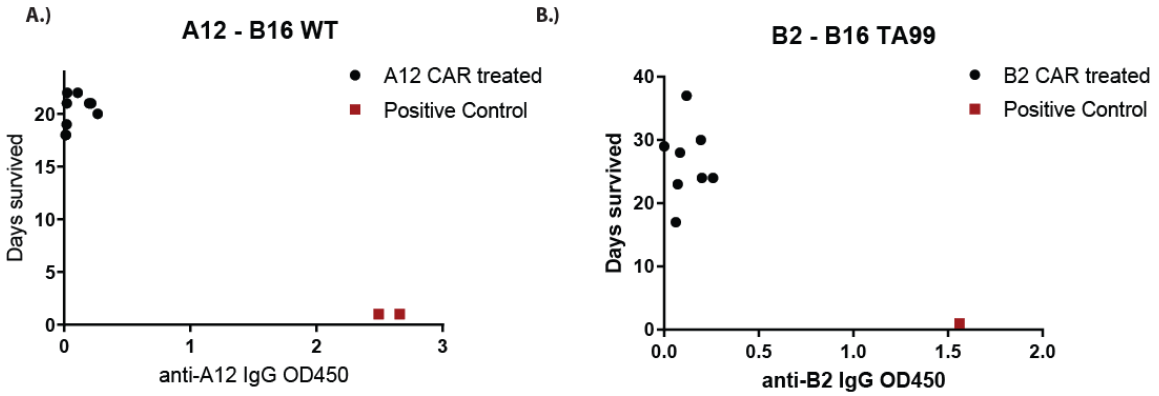

Fig. S4. VHH-based CAR T cells show low immunogenicity upon repeated administration. (A) Serum was harvested from B16-inoculated PD-L1-/- mice treated with A12 CARs. An anti-A12 VHH plated-based binding assay was run on the mouse serum to determine the level of anti-A12 IgGs produced. These anti-VHH IgG levels were compared to mice that have been actively immunized with A12 or mice that have been daily dosed with soluble VHH. The anti-A12 titers on CAR-treated mice is significantly lower than the positive anti-VHH serum samples, indicating low immunogenicity. Furthermore, the anti-VHH IgG levels from CAR-treated mice do not correlate with a survival detriment, indicating that immunogenicity is not a concern in our treatments. **(B)** Serum from WT B2-treated mice bearing B16 tumors was collected and analyzed for and anti-B2 response. Compared to a positive anti-VHH serum, the level of anti-B2 IgGs generated by repeated doses of B2 CAR T cell was low. Survival was not correlated to anti-B2 IgG level, suggesting anti-VHH immunogenicity was not a factor in the treatments.

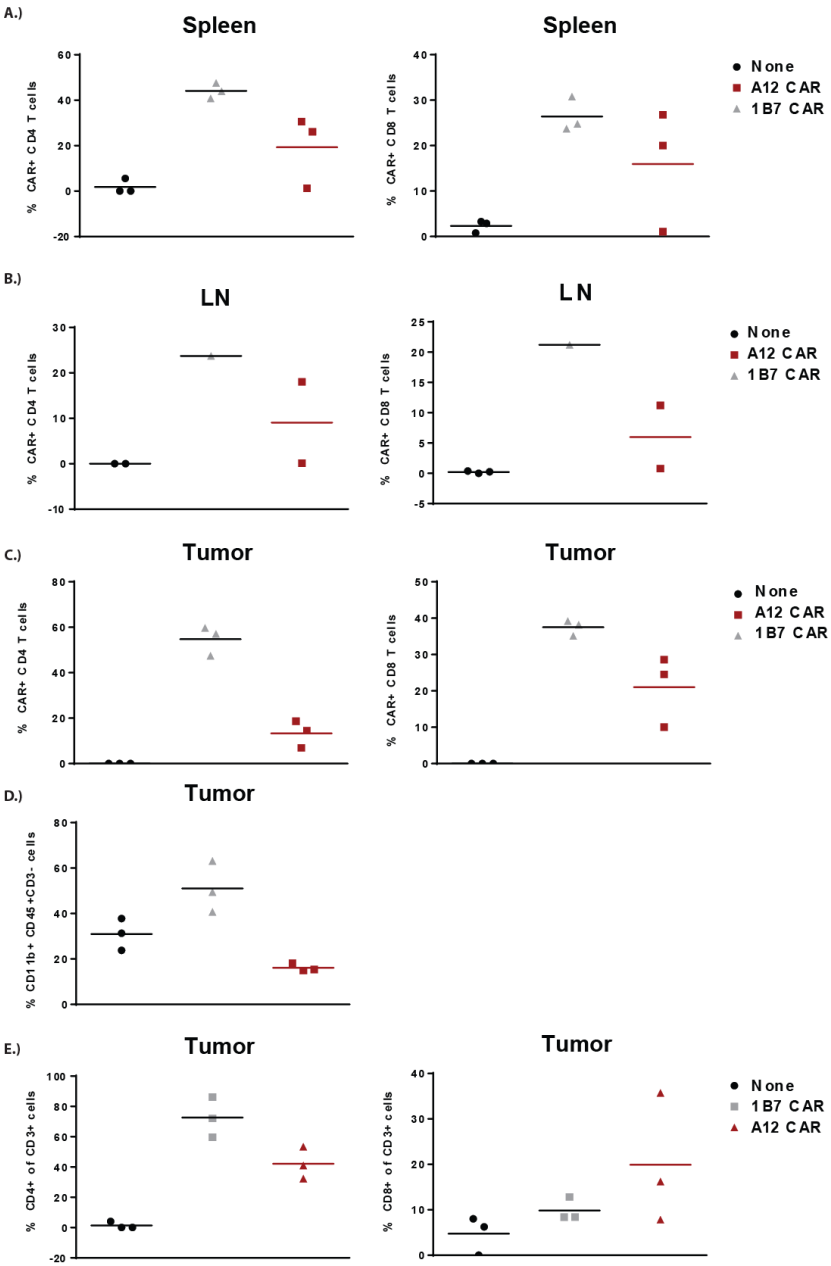

Fig. S5. A12 CAR T cells expand and persist in a RAG-/- background. The spleen **(A)**, tumor-draining lymph node **(B)**, and tumors **(C)** of RAG-/- mice treated with a single dose of A12 or 1B7 CAR T cells were harvested after the tumor areas reached 125 mm^2, and the presence of CAR-positive T cells was measured. CAR-positive T cells are present in the spleen, LN, and tumor, however the proportion of CAR-positive T cells was lower in the A12-treated mice, possibly indicating that the A12 CARs are becoming exhausted and less persistent. **(D)** The levels of CD11b+ cells in the tumors were measured, and the A12-treated mice showed the lowest level of CD11b+ cells. **(E)** The levels of CD4 and CD8 positive T cells in the tumor were analyzed, and the A12-treated mice showed an increase in the proportion of CD8 T cells compared to the 1B7-treated mice.

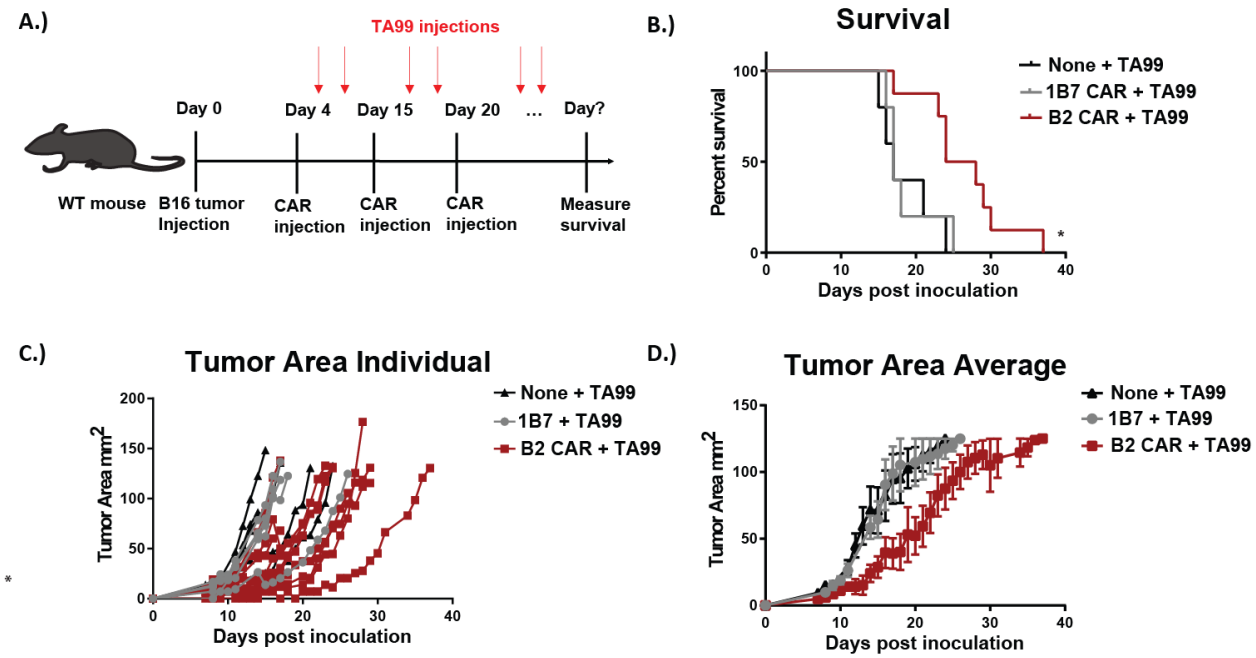

Fig. S6. B2 CAR T cells further delay tumor growth when combined with an anti-TRP1 antibody. (A) Schematic of *in vivo* experiments to test if TA99 combination treatment with B2 can further improve efficacy. Mice were treated with an anti-TRP1 antibody twice weekly in combination with either no CAR T cells, B2 CAR T cells or irrelevant 1B7 CAR T cells. **(B)** Kaplan-Meier curves measuring survival of each treatment group are shown. The B2 CAR T cell in combination with TA99 delayed tumor growth compared to TA99 treatment by itself or with a irrelevant CAR T cell ($p = 0.015$, log-rank Mantel Cox test). **(C)** The individual and **(D)** average tumor areas of each group were monitored and are shown.

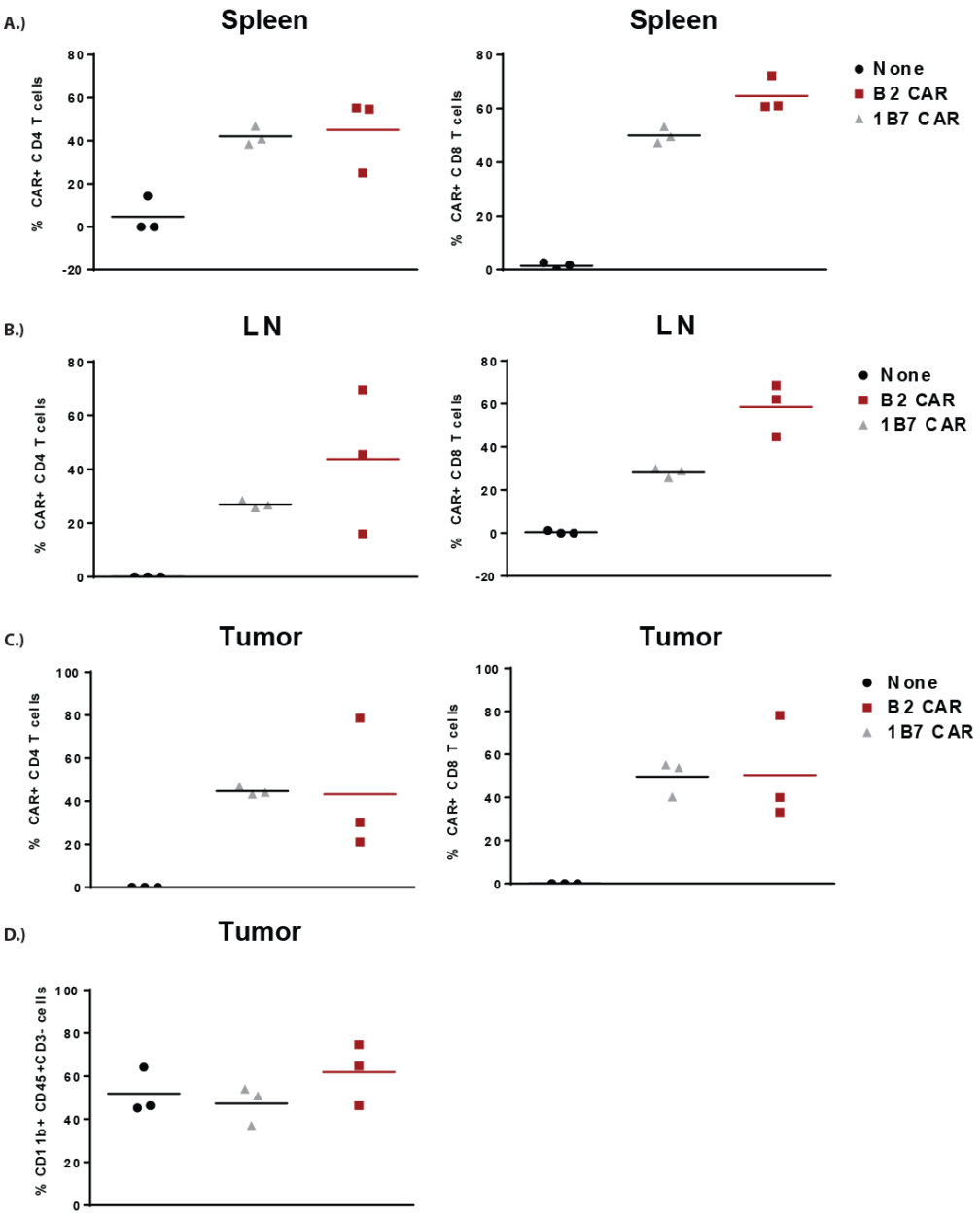

Fig. S7. B2 CAR T cells expand and persist in a RAG-/- background. The spleen **(A)**, tumor-draining lymph node **(B)**, and tumors **(C)** of RAG-/- mice treated with a single dose of B2 or 1B7 CAR T cells were harvested after the tumor areas reached 125 mm^2, and the presence of CAR-positive T cells was measured. CAR-positive T cells are present in the spleen, LN, and tumor, with slightly higher expansion of B2 cells in the LN compared to 1B7 cells in the LN. **(D)** The levels of CD11b+ cells in the tumors were measured, and the B2 and 1B7-treated mice showed comparable levels of CD11b+ cells.

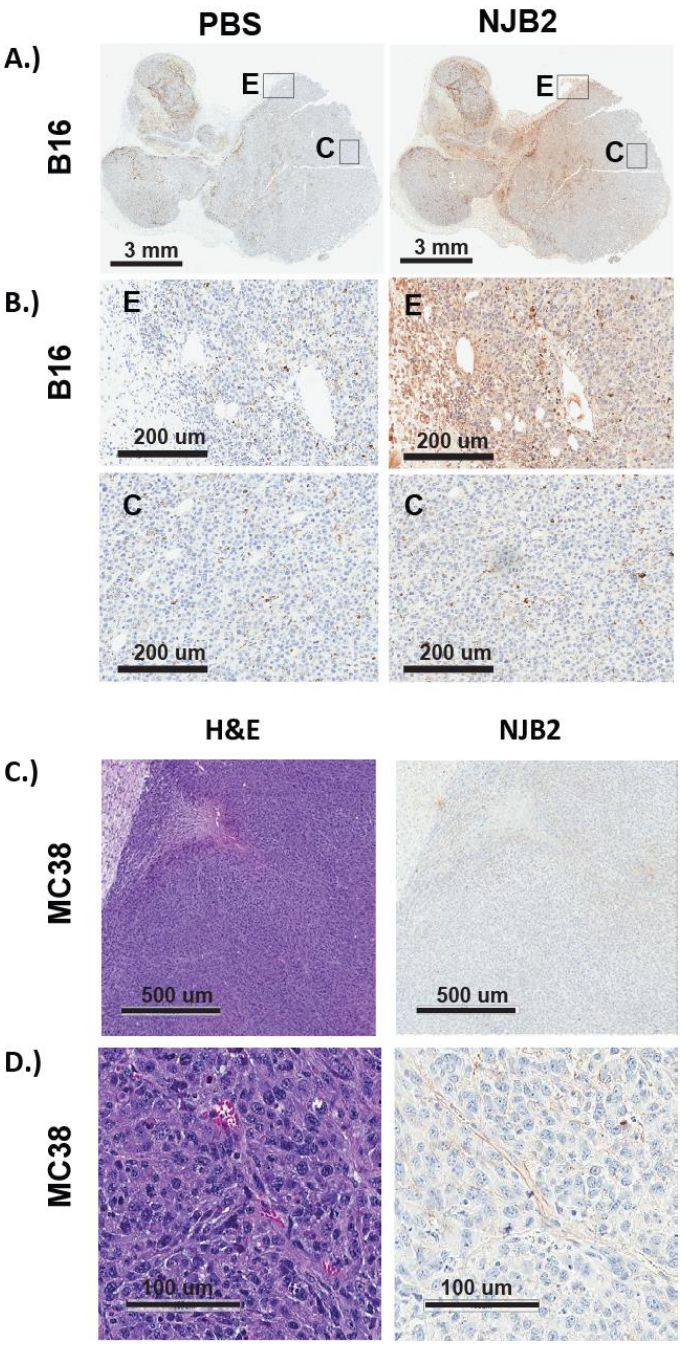

Fig. S8. MC38 tumors express less EIIIB than B16 tumors as recognized by the NJB2 VHH. Immunohistochemistry of B16 and MC38 shows less EIIIB in the tumor environment in MC38 tumors. B16 and MC38 tumors were excised and stained with biotinylated-B2 and detected with Streptavidin- horse radish peroxidase (HRP). **(A)** Left – IHC staining of B16 tumor at 0.8X magnification. Right – EIIIB staining of same B16 tumor. **(B)** 20X magnification of above panels showing an Edge (E) and Core (C) region **(C)** Left – H&E staining of MC38 tumor at magnification. Right – EIIIB staining of same MC38 tumor. **(D)** 5x magnification of above panels. Left – H&E staining of MC38 tumors. Right – EIIIB staining of MC38 tumor.

References

1. Rickelt S & Hynes RO (2018) Antibodies and methods for immunohistochemistry of extracellular matrix proteins. *Matrix biology : journal of the International Society for Matrix Biology*.
2. Jailkhani, N., Ingram, J.R., Rashidian, M., Rickelt, S., Ma, H., Tian, C., Jiang, Z., Ploegh, H. and Hynes, R.O. (2018). Non-invasive imaging of tumor progression, metastases and fibrosis using a nanobody targeting the extracellular matrix. *Proceedings of the National Academy of Sciences of the United States of America* (submitted)
3. Dougan M*, et al.* (2018) Targeting Cytokine Therapy to the Pancreatic Tumor Microenvironment Using PD-L1-Specific VHHs. *Cancer immunology research* 6(4):389-401.